Orthopaedics & Traumatology: Surgery & Research 104 (2018) 877–882

Available online at
ScienceDirect
www.sciencedirect.com

Elsevier Masson France
EM|consulte
www.em-consulte.com/en

Original article

Biomechanical comparison between stainless steel, titanium and carbon-fiber reinforced polyetheretherketone volar locking plates for distal radius fractures

Raffaele Mugnai [a,*], Luigi Tarallo [a], Francesco Capra [b], Fabio Catani [a]

[a] Orthopaedics and Traumatology Department, Modena University Hospital, Via Pietro Giardini, 1355, Baggiovara, 41126 Modena MO, Italy
[b] Rimini, Italy

ARTICLE INFO

Article history:
Received 2 March 2017
Received in revised form 18 January 2018
Accepted 16 May 2018

Keywords:
Distal radius
Plate
Bending stiffness
Load to failure
Biomechanical
Material

ABSTRACT

Introduction: As the popularity of volar locked plate fixation for distal radius fractures has increased, so have the number and variety of implants, including variations in plate design, the size and angle of the screws, the locking screw mechanism, and the material of the plates.
Hypothesis: Carbon-fiber reinforced polyetheretherketone (CFR-PEEK) plate features similar biomechanical properties to metallic plates, representing, therefore, an optimal alternative for the treatment of distal radius fractures.
Materials and Methods: Three different materials-composed plates were evaluated: stainless steel volar lateral column (Zimmer); titanium DVR (Hand Innovations); CFR-PEEK DiPHOS-RM (Lima Corporate). Six plates for each type were implanted in sawbones and an extra-articular rectangular osteotomy was created. Three plates for each material were tested for load to failure and bending stiffness in axial compression. Moreover, 3 constructs for each plate were evaluated after dynamically loading for 6000 cycles of fatigue.
Results: The mean bending stiffness pre-fatigue was significantly higher for the stainless steel plate. The titanium plate yielded the higher load to failure both pre and post fatigue. After cyclic loading, the bending stiffness increased by a mean of 24% for the stainless steel plate; 33% for the titanium; and 17% for the CFR-PEEK plate. The mean load to failure post-fatigue increased by a mean of 10% for the stainless steel and 14% for CFR-PEEK plates, whereas it decreased (−16%) for the titanium plate. Statistical analysis between groups reported significant values ($p < 001$) for all comparisons except for Hand Innovations vs. Zimmer bending stiffness post fatigue ($p = .197$).
Discussion: The significant higher load to failure of the titanium plate, makes it indicated for patients with higher functional requirements or at higher risk of trauma in the post-operative period. The CFR-PEEK plate showed material-specific disadvantages, represented by little tolerance to plastic deformation, and lower load to failure.
Level of evidence: N/A.

1. Introduction

As the popularity of volar locked plate fixation for distal radius fractures has increased, so have the number and variety of implants, including variations in plate design [1–4], the size and angle of the screws [1], the locking screw mechanism [5], and the material of the plates [6].

In the past few decades, the use of titanium alloys has gained popularity, because of its excellent biocompatibility, high mechanical strength and corrosion resistance [7]. A potential advantage of titanium alloy plates (e.g. Ti–6Al–4 V) is represented by the less stress-shielding to bone, because its stiffness is 110 ± 10 GPa [8,9], compared to 200 ± 20 GPa of stainless steel (e.g. 316 L) [10], but much higher, however, than that of human cortical bone (around 20 GPa) [11]. Disadvantages of metal implants include limited fatigue life, mismatch of modulus of elasticity, cold-welding seen with titanium locking screw constructs, corrosion, osseo-integration, and radiodensity that can preclude accurate

* Corresponding author.
E-mail address: raffaele.mugnai@gmail.com (R. Mugnai).

https://doi.org/10.1016/j.otsr.2018.05.002
1877-0568/

radiographic visualization of fracture reduction, healing, and tumor or infection progression or resolution [12,13].

"Semi-rigid" Carbon-Fiber Reinforced (CFR) polymers fracture fixation plates were developed starting in the 1980s as an alternative to comparatively "rigid" metallic bone plates [14,15].

In literature, several studies reported the biomechanical properties of CFR implants [16–19]; however, only few recent studies directly compared the biomechanical characteristics of metallic and CFR polymer bone plates [19–21].

Thus, the aim of the present research was to compare the load to failure and bending stiffness with a single axial load and after cyclical loading of three different materials-composed plates currently available for distal radius fractures. It was our hypothesis that the Carbon-Fiber Reinforced polyetheretherketone (CFR-PEEK) plate would feature similar biomechanical properties in terms of load to failure with reduced stiffness, compared with titanium and stainless steel plates, therefore representing an optimal choice for the treatment of distal radius fractures.

2. Materials and Methods

2.1. Specimens preparation

The fixed-angle volar plating systems tested were: stainless steel volar lateral column (Zimmer, Warsaw, IN); titanium DVR (Hand Innovations, Miami, FL); CFR-PEEK DiPHOS-RM (Lima Corporate, San Daniele Del Friuli, Udine, Italy). Six plates were obtained from each individual manufacturer through research donation. For each type of plate, 6 right synthetic composite bone radii with a cancellous inner core and a foam cortical shell (25 cm long, 5.5 mm canal diameter; model #1027-20, Pacific Research Laboratories, Inc., Vashon, WA, USA) were used. Plates were implanted using all the distal and proximal fixation holes (Fig. 1). The CFR-PEEK plate featured the possibility of minimal variable axis for the distal screws. However, in our research neutral orientation of the distal screws was assured by inserting the guide sleeve in the specfic alignment mask. The remaining two plates (stainless steel volar lateral column and titanium DVR) incorporated a fixed screw axis.

An unstable, extraarticular fracture was simulated by making an 8 mm gap with a saw starting 12 mm proximal to the articular surface of the radius on the distal radio-ulnar joint side. The osteotomies were made perpendicular to the long axis of the bone to allow for a consistent fracture gap on the dorsal and volar sides of the radius. We decided to perform a rectangular osteotomy, allowing to focus on the loads transmitted to the plate, since we hypothesized that a wedge osteotomy with partial bone contact on the dorsal side could influence the resistance of the fracture gap motion [22,23]. A single investigator (L.T.) created the fractures and applied all the plates to minimize variability. The proximal 15 cm of each synthetic radius model were potted in methylmethacrylate. In order to ensure standardised axial load transfer, each radius was fixed in line with its long axis from the radial part of the lunate fossa to the centre of the head of the radius, to provide for linear load transfer; then the potting cup was secured in the testing machine.

2.2. Tests description

Three plates for each type were tested for load to failure and bending stiffness pre-fatigue using a bi-axial servo-hydraulic test frame (MTS Minibionix 858, universal testing machine) by advancing a ceramic sphere, centered at the radial side of the lunate fossa, at a constant rate of displacement of 5 mm/min [22] (Fig. 2). The failure load was defined as the first local maximum of the

Fig. 1. Plates tested. From left to right: titanium DVR (Hand Innovations, Miami, FL); CFR-PEEK DiPHOS-RM (Lima Corporate, San Daniele Del Friuli, Udine, Italy); stainless steel volar lateral column (Zimmer, Warsaw, IN).

Fig. 2. Axial loading test performed by advancing a ceramic sphere centered over the lunate fossa at a constant rate of displacement of 5 mm/min.

Table 1
Bending stiffness and load to failure for each type of plate evaluated.

	Bending Stiffness	mean ± SD (N/mm)		Load to Failure	mean ± SD (N)	
	Pre-fatigue	Post-fatigue	*p*	Pre-fatigue	Post-fatigue	*p*
Stainless steel	153.6 ± 1.9	190.4 ± 4.3	0.004	431.3 ± 8.5	472.3 ± 6.1	0.021
Titanium	139.3 ± 4.7	186.0 ± 1.7	0.001	786.3 ± 5.7	675.0 ± 4.0	0.002
CFR-PEEK	123.4 ± 3.6	143.8 ± 1.5	0.002	389.7 ± 5.7	444.0 ± 7.9	0.016

force-displacement curve. This measure was automatically computed by finding the first data point where the slope of the curve dropped to zero, corresponding with plate damage (bent or broken).

The bending stiffness was defined as the slope of the regression line within the elastic range. The elastic range was found by iteratively adding data points to a linear regression analysis until the coefficient of determination reached its maximum ($R^2 > .998$ for all samples) [24,25].

Moreover, 3 constructs for each plate were dynamically loaded for 6000 cycles of fatigue [6] at a frequency of 10 Hz, with a load value corresponding to 50% of the previously calculated load to failure. According with Steinberg et al. [19], we decided to use a material specific load target to prevent an eventual premature failure under cyclic fatigue loading, as the mechanisms associated with fatigue-crack propagation in brittle materials (i.e. polymers) are quite distinct from those commonly encountered in metals; in particular, the crack-growth rate behaviour in brittle materials displays a markedly higher sensitivity to the applied stress intensity than is observed in most metals [26]. Finally, the 3 constructs were loaded to failure, as previously described, measuring the load to failure and bending stiffness post-fatigue.

2.3. Statistics

Absolute frequency and percentage were calculated for categorical data, while mean ± standard deviation (SD) were used for continuous data. The paired sample *t*-test was employed to evaluate the pre and post-fatigue differences in terms of bending stiffness and load to failure for each plate; while the comparison between the three plates tested was performed with ANOVA. MedCalc version 11.5.1 (MedCalc Software, Mariakerke, Belgium) was used for the analysis. P values were considered statistically significant if smaller than 0.05.

3. Results

The mean bending stiffness pre-fatigue was significantly higher for the stainless steel plate (153.6 ± 1.9 N/mm), in comparison to titanium plate (139.3 ± 4.7 N/mm), and CFR-PEEK plate (123.4 ± 3.6 N/mm) (Table 1). The mean load to failure pre-fatigue was 431.3 ± 8.5 N for the stainless steel plate, 786.3 ± 5.7 N for the titanium plate, and 389.7 ± 5.7 N for the CFR-PEEK plate (Table 1) (Fig. 3), and these differences reached statistical significance.

All fracture constructs survived all phases of the cyclic loading testing. After cyclic loading, the bending stiffness significantly increased by a mean 24% for the stainless steel (190.4 ± 4.3 N/mm); 33% for the titanium (186.0 ± 1.7 N/mm); and 17% for the CFR-PEEK plate (143.8 ± 1.5 N/mm) (Figs. 4 and 5). The mean load to failure post-fatigue produced an increased value corresponding to 10% for the stainless steel (472.3 ± 6.1 N) and 14% for CFR-PEEK (444.0 ± 7.9 N) plates, whereas it decreased (−16%) for the titanium (675.0 ± 4.0 N) plate (Fig. 5) (Table 1). One-way analysis of variance for independent samples was performed to evaluate differences between the three plates tested; statistical analysis between groups reported significant values ($p < 001$) for all comparisons except for one bending stiffness – Hand Innovations vs Zimmer post fatigue ($p = .197$), which therefore showed no significant statistical differences. No cases of screws loosening were reported.

4. Discussion

Our results suggest that the titanium plate yields the higher load to failure value both pre and post-fatigue, followed by stainless

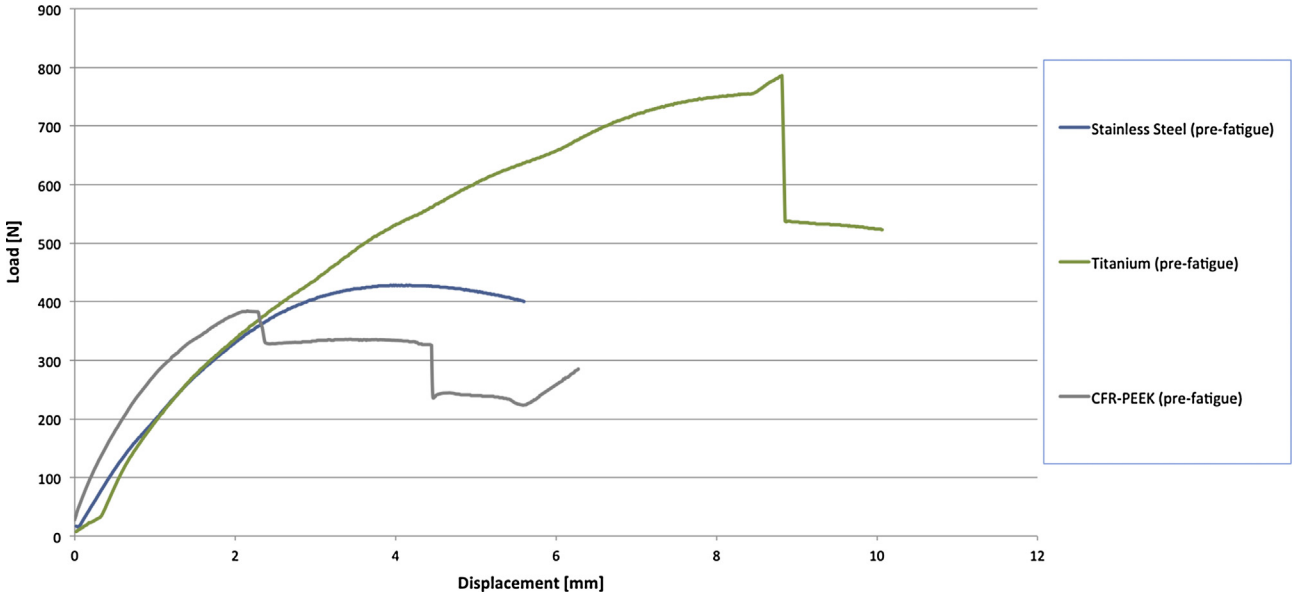

Fig. 3. Force-displacement curves (mean of the three tests for each type of plate) pre-fatigue.

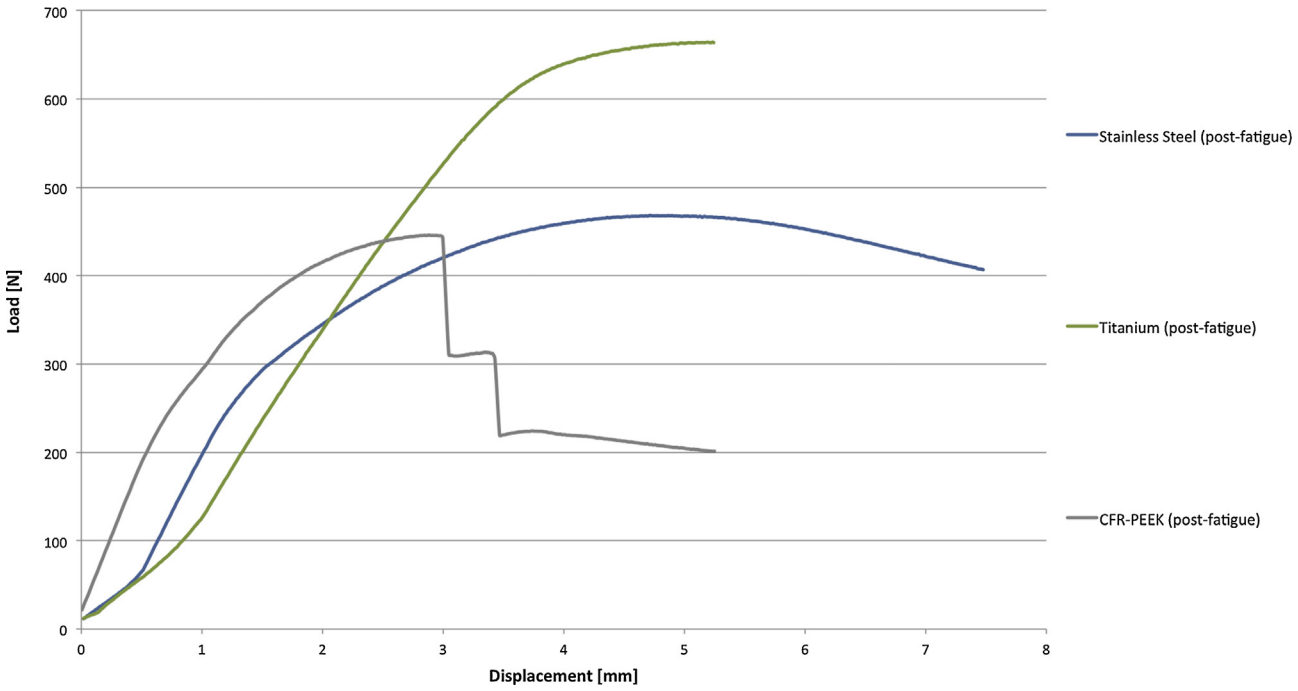

Fig. 4. Force-displacement curves (mean of the three tests for each type of plate) post-fatigue.

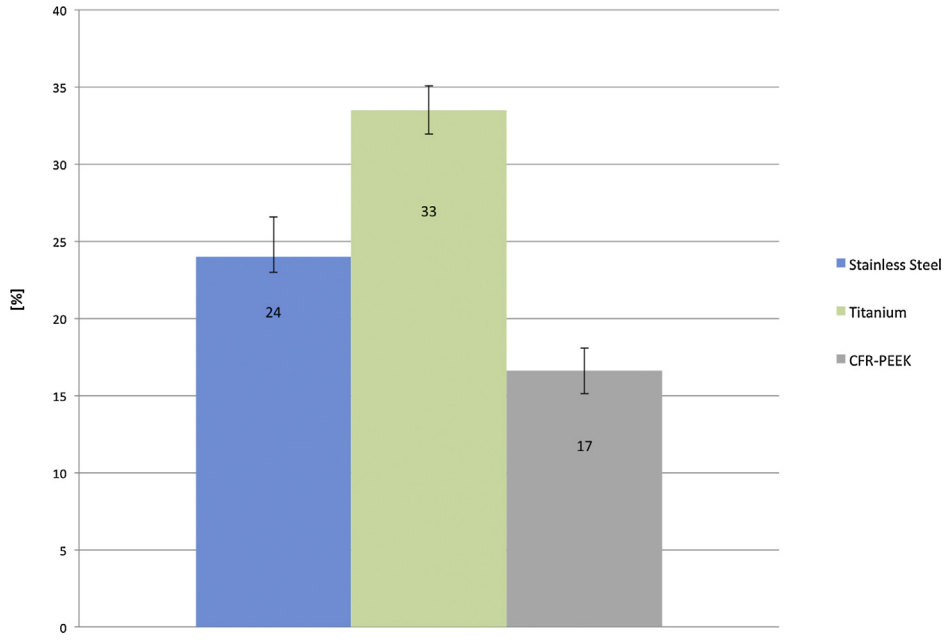

Fig. 5. Mean bending stiffness post-fatigue increment.

steel and CFR-PEEK plates. Similarily to our results, Sobky et al. compared the load to failure between the titanium DVR plate (Hand Innovations), SCS/V (Avanta), Lo-Con VLS plate (Wright Medical), and volar radius stainless locking plate (Synthes), implanted in left sawbone radii, obtaining significantly higher load to failure for the titanium DVR plate [2].

Several animal [27] and human [28–31] studies demonstrated that rigid plates can cause bone loss underneath the plates with increased risk of refracture after plate removal. However, according with the results of previous studies [17,19,21], a potential disadvantage of the CFR-PEEK plate is represented by the little tolerance to plastic deformation, resulting in implant breakage when the force applied exceeds the load to failure.

In particular, we observed during both pre and post-fatigue axial loading tests that breakage line of the CFR-PEEK plate always occurred at the proximal row holes on the head portion of the plate (Fig. 6). Recent studies have evaluated the bending stiffness of different plate designs and materials [2,6,19,20,32–35]. Dahl et al. compared the yield strenghts and bending stiffness under graduated cyclic loading conditions (100 N, 200 N, 300 N, and loaded for 2000 cycles of fatigue in each phase for a total of 6000 cycles) between 8 different plates for the treatment of

Fig. 6. CFR-PEEK plate breakage line at the proximal row holes on the head portion of the plate during both pre and post-fatigue axial loading tests.

distal radius fractures: Acu-Loc (Acumed, Hillsboro, OR), DVR (Hand Innovations, Miami, FL), SCS volar distal radial plate (Small Bone Innovations, Morrisville, PA), volar distal radius plate and EA extra-articular volar distal radius plate (Synthes, Paoli, PA), Matrix-Smart-Lock (Stryker Leibinger, Kalamazoo, MI), Locon VLS (Wright Medical Technology, Arlington, TN), and periarticular distal radius locking plate (Zimmer, Warsaw, IN), implanted in synthetic composite radii [32]. The mean initial stiffness of all plates at a load of 100 N was approximately 150 N/mm. The Wright plate showed significantly higher stiffness at 100 N load compared to the Zimmer plate. All 8 plates showed increasing stiffness at higher loads. In particular the Zimmer plate was more compliant both at 100 N, 200 N, and 300 N than the Hand Innovations plate [32].

These findings differ from the results of our study, were the titanium Hand Innovations plate showed less bending stiffness both pre and post fatigue axial loading tests than the stainless steel Zimmer plate. However, after cyclic loading, the bending stiffness revealed an higher increase (+33%) for the Hand Innovations, with respect to the Zimmer (+24%) plate. The high increase in the bending stiffness after cyclic loading showed by the titanium plate may be a possible explanation for these different results, as in the study of Dahl et al. [32], all the axial loading tests were performed under graduated cyclic loading conditions, emphasizing, therefore, the effect of this possible "strain hardening" mechanism [36].

The present research has a number of inherent limitations. The first is represented by the difference in implant shape, size and thickness that will inevitably contribute to differences in biomechanical performances. Moreover, we evaluated the bending stiffness and load to failure only under axial compression, not including volar/dorsal bending and torsional loading conditions.

Future studies are required to evaluate the biomechanical properties of these different plate materials for volar plate fixation of distal radius fracture including volar/dorsal bending and torsional loading tests and to investigate the possible explanation of the reduction in the load to failure after fatigue tests for the Hand Innovations titanium plate.

5. Conclusions

The results of the present study may provide useful information for physicians when choosing among different plate materials for the treatment of distal radius fractures. Titanium plate demonstrated significantly more strength in peak load to failure and failure after fatigue cycling. The CFR-PEEK yields material-specific advantages, including X-rays radiolucency, easier implant removal, avoiding the "cold welding" phenomenon, and lower bending stiffness. However, disadvantages of this plate are represented by the little tolerance to plastic deformation, with the risk of implant breakage, and the lower load to failure with respect to the other materials evaluated. Therefore, proper patient selection (avoiding incompliant or non collaborative) should be performed using when using this plate to avoid possible implant breakage consequent to a fall or a second trauma on the injured wrist until the complete fracture healing.

Disclosure of interest

The authors declare that they have no competing interest.

Funding

This research did not receive any specific grant from funding agencies in the public, commercial, or not-for-profit sectors. The plates tested in this study were provided through research donation from the following companies: Biomet (Hand Innovations titanium DVR), Zimmer (stainless steel volar lateral column), and Lima Corporate (CFR-PEEK DiPHOS-RM).

Authors' contributions

All authors should have made substantial contributions to all of the following: (1) the conception and design of the study, or acquisition of data, or analysis and interpretation of data, (2) drafting the article or revising it critically for important intellectual content, (3) final approval of the version to be submitted. In particular, Dott. R. Mugnai, Dott. L. Tarallo, and Dott. F. Catani designed the study. Dott R. Mugnai was responsible for data collection. Dott. F. Capra was responsible for data analysis. Dott. F. Catani contributed to interpretation of data. Dott. R. Mugnai drafted the manuscript, together Dott. L. Tarallo. All authors critically revised the manuscript. All authors read and approved the final manuscript.

References

[1] Mudgal CS, Jupiter JB. Plate and screw design in fractures of the hand and wrist. Clin Orthop Relat Res 2006;445:68–80.

[2] Sobky K, Baldini T, Thomas K, Bach J, Williams A, Wolf JM. Biomechanical comparison of different volar fracture fixation plates for distal radius fractures. Hand (NY) 2008;3:96–101.
[3] Evans S, Ramasamy A, Deshmukh SC. Distal volar radial plates: how anatomical are they? Orthop Traumatol Surg Res 2014;100:293–5.
[4] Obert L, Rey PB, Uhring J, Gasse N, Rochet S, Lepage D, et al. Fixation of distal radius fractures in adults: a review. Orthop Traumatol Surg Res 2013;99:216–34.
[5] Egol KA, Kubiak EN, Fulkerson E, Kummer FJ, Koval KJ. Biomechanics of locked plates and screws. J Orthop Trauma 2004;18:488–93.
[6] Marshall T, Momaya A, Eberhardt A, Chaudhari N, Hunt TR. 3rd. Biomechanical Comparison of Volar Fixed-Angle Locking Plates for AO C3 Distal Radius Fractures: Titanium Versus Stainless Steel With Compression. J Hand Surg Am 2015;40:2032–8.
[7] Smith LJ, Swaim JS, Yao C, Haberstroh KM, Nauman EA, Webster TJ. Increased osteoblast cell density on nanostructured PLGA-coated nanostructured titanium for orthopedic applications. Int J Nanomedicine 2007;2:493–9.
[8] Disegi JA. Titanium alloys for fracture fixation implants. Injury 2000;31:S14–7.
[9] Golish SR, Mihalko WM. Principles of biomechanics and biomaterials in orthopaedic surgery. J Bone Joint Surg Am 2011;93:207–12.
[10] Disegi JA, Eschbach L. Stainless steel in bone surgery. Injury 2000;31:S2–6.
[11] Bayraktar HH, Morgan EF, Niebur GL, Morris GE, Wong EK, Keaveny TM. Comparison of the elastic and yeld properties of human femoral trabecular and cortical bone tissue. J Biomech 2004;37:27–35.
[12] Suzuki T, Smith WR, Stahel PF, Morgan SJ, Baron AJ, Hak DJ. Technical problems and complications in the removal of the less invasive stabilization system. J Orthop Trauma 2010;24:414–9.
[13] Van Nortwick SS, Yao J, Ladd AL. Titanium integration with bone, welding, and screw head destruction complicating hardware removal of the distal radius: report of 2 cases. J Hand Surg Am 2012;37:1388–9.
[14] Bradley JS, Hastings GW, Johnson-Nurse C. Carbon fibre reinforced epoxy as a high strength, low modulus material for internal fixation plates. Biomaterials 1980;1:38–40.
[15] Tayton K, Johnson-Nurse C, McKibbin B, Bradley J, Hastings G. The use of semi-rigid carbon fibre-reinforced plastic plates for fixation of human fractures. Results of preliminary trials. J Bone Joint Surg Br 1982;64:105–11.
[16] Hak DJ, Mauffrey C, Seligson D, Lindeque B. Use of carbon-fiber-reinforced composite implants in orthopedic surgery. Orthopedics 2014;37:825–30.
[17] Bagheri ZS, El Sawi I, Schemitsch EH, Zdero R, Bougherara H. Biomechanical properties of an advanced new carbon/flax/epoxy composite material for bone plate applications. J Mech Behav Biomed Mater 2013;20:398–406.
[18] Li CS, Vannabouathong C, Sprague S, Bhandari M. The use of carbon-fiber-reinforced (CFR) PEEK material in orthopedic implants: a systematic review. Clin Med Insights Arthritis Musculoskelet Disord 2015;23:33–45.
[19] Steinberg EL, Rath E, Shlaifer A, Chechik O, Maman E, Salai M. Carbon fiber reinforced PEEK Optima-a composite material biomechanical properties and wear/debris characteristics of CF-PEEK composites for orthopedic trauma implants. J Mech Behav Biomed Mater 2013;17:221–8.
[20] Katthagen JC, Schwarze M, Warnhoff M, Voigt C, Hurschler C, Lill H. Influence of plate material and screw design on stiffness and ultimate load of locked plating in osteoporotic proximal humeral fractures. Injury 2016;47:617–24.
[21] Wilson WK, Morris RP, Ward AJ, Carayannopoulos NL, Panchbhavi VK. Torsional failure of carbon fiber composite plates versus stainless steel plates for comminuted distal fibula fractures. Foot Ankle Int 2016;37(5):548–53.
[22] Kim SJ, Jo JH, Choi WS, Lee CH, Lee BG, Kim JH, et al. Biomechanical Properties of 3-Dimensional Printed Volar Locking Distal Radius Plate: Comparison With Conventional Volar Locking Plate. J Hand Surg Am 2017;42:747 [e1-e6].
[23] Hart A, Collins M, Chhatwal D, Steffen T, Harvey EJ, Martineau PA. Can the use of variable-angle volar locking plates compensate for suboptimal plate positioning in unstable distal radius fractures? A biomechanical study. J Orthop Trauma 2015;29:e1–6.
[24] Osada D, Fujita S, Tamai K, Iwamoto A, Tomizawa K, Saotome K. Biomechanics in uniaxial compression of three distal radius volar plates. J Hand Surg Am 2004;29:446–51.
[25] Kamei S, Osada D, Tamai K, Kato N, Takai M, Kameda M, et al. Stability of volar locking plate systems for AO type C3 fractures of the distal radius: biomechanical study in a cadaveric model. J Orthop Sci 2010;15:357–64.
[26] Ritchie RO. Mechanisms of fatigue-crack propagation in ductile and brittle solids. Int J Fract 1999;100:55–83.
[27] Tonino AJ, Davidson CL, Klopper PJ, Linclau LA. Protection from stress in bone and its effects: experiments with stainless steel and plastic plates in dogs. J Bone Joint Surg Br 1976;58:107–13.
[28] Janes GC, Collopy DM, Price R, Sikorski JM. Bone density after rigid plate fixation of tibial fractures. A dual-energy X-ray absorptiometry study. J Bone Joint Surg Br 1993;75:914–7.
[29] Kettunen J, Kröger H, Bowditch M, Joukainen J, Suomalainen O. Bone mineral density after removal of rigid plates from forearm fractures: preliminary report. J Orthop Sci 2003;8:772–6.
[30] Patman LJ, Szalay EA. Relative osteopenia after femoral implant removal in children and adolescents. Orthopedics 2013;36:e468–72.
[31] Terjesen T, Nordby A, Arnulf V. Bone atrophy after plate fixation: computed tomography of femoral shaft fractures. Acta Orthop Scand 1985;56:416–8.
[32] Dahl WJ, Nassab PF, Burgess KM, Postak PD, Evans PJ, Seitz WH, et al. Biomechanical properties of fixed-angle volar distal radius plates under dynamic loading. J Hand Surg Am 2012;37:1381–7.
[33] Meeson RL, Goodship AE, Arthurs GI. A biomechanical evaluation of a Hybrid Dynamic Compression Plate and a CastLess Arthrodesis Plate for pancarpal arthrodesis in dogs. Vet Surg 2012;41:738–44.
[34] Sakai A, Oshige T, Zenke Y, Menuki K, Murai T, Nakamura T. Mechanical comparison of novel bioabsorbable plates with titanium plates and small-series clinical comparisons for metacarpal fractures. J Bone Joint Surg Am 2012;94:1597–604.
[35] Willis AA, Kutsumi K, Zobitz ME, Cooney WP. 3rd. Internal fixation of dorsally displaced fractures of the distal part of the radius. A biomechanical analysis of volar plate fracture stability. J Bone Joint Surg Am 2006;88:2411–7.
[36] Sakai T, Belyakov A, Kaibyshev R, Miura H, Jonas JJ. Dynamic and post-dynamic recrystallization, under hot, cold and severe plastic deformtion conditions. Prog Mater Sci 2014;60:130–207.